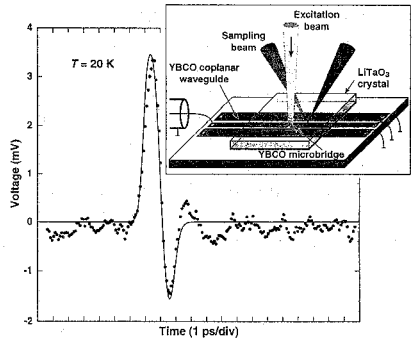

CTuC8 Fig. 1 Measured transient (dots) at $T = 20$ K and the results from the simulation (solid line). The inset shows the sample configuration and the electro-optic sampling beams.

$LiTaO_3$ crystal to facilitate the EO sampling measurements. The detector was excited and EO probed with ~100-fs-wide pulses from a Ti:sapphire laser. The 400-nm wavelength excitation with ~60-μW average power was delivered directly to the microbridge, while the generated electrical pulse was probed with an 800-nm wavelength beam only ~20 μm from the detector element. During the measurements, the microbridge was inside an exchange-gas, liquid-helium dewar, current-biased in the superconducting state through a microwave bias-tee.

We observed a ~1-ps-wide transient of the shape shown in Fig. 1 (dots). This bipolar signal is characteristic for the nonequilibrium kinetic inductive response.[1] Nearly identical waveforms, in terms of their temporal characteristics were observed for all bias currents less than the bridge critical current in the temperature range from 20–80 K.

Nonequilibrium conditions govern the observed photoresponse and can be accurately modeled by the Rothwarf-Taylor (R-T) equations—two coupled differential equations which describe the interplay between the quasiparticles and the phonons.[6,7] The solid line in Fig. 1 shows the R-T fit to the measured transient. From our experiments we can extract the subpicosecond time constants, which can be regarded as the intrinsic speed for a YBCO kinetic inductive photodetector. The mechanism for the photoresponse is spectrally very broadband and detection from ultraviolet to 10 μm wavelengths has been experimentally demonstrated.[4,5] Our studies prove the high-speed capabilities of YBCO photodetectors, and are opening the door to many interesting applications in the area of superconducting optoelectronics. It is expected that YBCO fiber-optic communication receivers with Gbit/s rates find applications as ultrafast optical-to-electrical transducers for superconducting digital electronics using rapid single-flux quantum circuits and for high-speed data transmission in the cryogenic environment.

This research was supported by the Office of Naval Research grant N00014-96-1-1027. C. W. acknowledges support from the U.S. Army Research Office AASERT grant DAAH04-95-1-0428.

**Brockhouse Institute for Materials Research, McMaster University, Hamilton, Ontario L8S 4M1, Canada*

***Quantum Institute, University of California, Santa Barbara, California 93106-5100*

1. N. Bluzer, Phys. Rev. B **44,** 10222 (1991).
2. F. A. Hegmann, D. Jacobs-Perkins, C.-C. Wang, S. H. Moffat, R. A. Hughes, J. S. Preston, M. Currie, P. M. Fauchet, T. Y. Hsiang, R. Sobolewski, Appl. Phys. Lett. **67,** 285 (1995).
3. M. Lindgren, M. A. Zorin, V. Trifonov, M. Danerud, D. Winkler, B. S. Karasik, G. N. Gol'tsman, E. M. Gershenzon, Appl. Phys. Lett. **65,** 3398 (1994).
4. V. A. Trifonov, B. S. Karasik, M. A. Zorin, G. N. Gol'tsman, E. M. Gershenzon, M. Lindgren, M. Danerud, D. Winkler, Appl. Phys. Lett. **68,** 1418 (1996).
5. M. Lindgren, M. Currie, C. Williams, T. Y. Hsiang, P. M. Fauchet, Roman Sobolewski, S. H. Moffat, R. A. Hughes, J. S. Preston, F. A. Hegmann, to appear in Phys. Rev. Lett. (1996).
6. A. Rothwarf and B. N. Taylor, Phys. Rev. Lett. **19,** 27 (1967).
7. C. C. Chi, M. M. T. Loy, D. C. Cronemeyer, Phys. Rev. B **23,** 124 (1981).

CTuD

8:00 am–10:00 am
Rooms 321/323

Optical Studies of Cell Properties

Alexander M. Sergeev, *Institute of Applied Physics, Russia, Presider*

CTuD1 (Invited) 8:00 am

Time-resolved x-ray microscopy in biology and medical science

Martin C. Richardson, *Laser Plasma Laboratory, CREOL, University of Central Florida, 4000 Central Florida Blvd., PO Box 162700, Orlando, Florida 32816-2700; E-mail: mcr@mail.creol.ucf.edu*

X-ray microscopy offers several inherent advantages for the biological and medical sciences over other high-resolution microscopy techniques, such as confocal optical microscopy and electron microscopy.[1] Short wavelength radiation allows for much higher spatial resolution than optical techniques, while at the same time possessing sufficient depth of field to image whole-cell structures of several microns size. High image contrast, and even elemental mapping, can be obtained by selection of the appropriate x-ray wavelength. Moreover in avoiding the need for the sample preparation procedures inherent to electron microscopy (staining, drying, sectioning etc.) x-ray imaging permits the visualization of biological specimens in their natural state. Previous developments in x-ray microscopy have mostly used synchrotron radiation sources.[2–4] These offer precision variability in x-ray emission but are restricted to major facilities, and require long exposure times to record an image. This latter limitation prevents the high resolution analysis of mobile living organisms.[5] Early work with laser plasma x-ray sources also required the use of major facilities.[6]

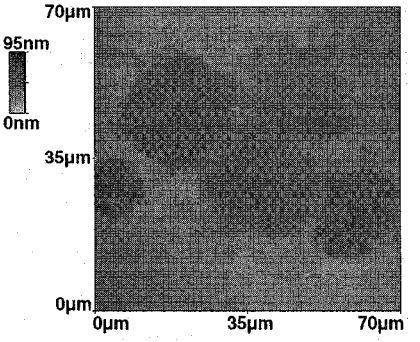

CTuD1 Fig. 1 Image of mouse macrophages.

We believe we present the first demonstration of single-frame x-ray imaging of biological specimens in their natural state, made with a compact solid-state laser plasma source. Specimens such as live mouse macrophages,[7] lipopolysaccharide (LPS)[8] from *Burkholderia cepacia,* soft muscle tissue[9] and others were analyzed were used as specimens. By adjustment of the target and irradiation conditions, the laser-produced plasma can be spectrally tailored to emit preferentially in specific regions. For instance, laser plasmas produced from yttrium targets emit mostly in the water window region (2.3–4.4 nm), more suitable for high contrast imaging of smaller biological specimens, like viruses, whereas laser plasmas generated from gold targets emit in a broader band, a better choice for imaging fine details on larger organisms.[10] Selection of specific combinations of target and filtering materials, produces narrow spectral lines of x-rays that can be tailored to the absorption of elements to be identified. The ultrashort duration of laser plasma x-rays permits single-shot framed images to be recorded in times much shorter than any kinetic response of biological organisms, including those produced by the x-ray radiation.[11] Thus the images obtained by this method portray the organism in its natural state, unaltered by preparation or radiation.

The contact x-ray microscopy method[5] is simple in procedure. The specimen is placed on an x-ray resist, Polymethylmethacrylate (PMMA), supported by a silicon base inside a sample holder containing an x-ray window, designed to protect wet specimens within vacuum. The laser plasma is produced by a Nd:glass laser producing 10–20 J of 1064-nm light in a 5-ns pulse. The irradiated area on the targets is approximately 100 μm in diameter. The intensity on the targets reaches 5×10^{13} W/cm^2. The pulse width of the x-ray emission, in the water widow region (2.3–4.4 nm), is approximately the same as the laser pulse width. The specimen holder is placed 1 cm away from the target, at an angle of 45°, from the target normal. A single x-ray exposure is made for each specimen. The photo x-ray resist is then developed and analyzed with an atomic force microscope.

A typical image of thioglycollaate elicited macrophages obtained from BALB/c mouse peritoneal cavity is shown in Fig. 1. Macrophages are professional phagocytic cells capable of ingesting and destroying antigens. This figure shows an x-ray image of live, unfixed, macrophage cells suspended in tissue

culture medium. Comparisons of images of these specimens with those that have been fixed, and those that have been analyzed with electron microscopy show marked differences.

In this talk, examples of x-ray images obtained of other organisms in these material state are given. In addition, the development of techniques to analyze the time dependence of specific effects (such as the effects of structurally-modifying drugs), and progress towards achieving single-shot, real-time imaging of biological specimens using laser-plasma x-ray sources will be described.

This work was supported by AFOSR through contract #F49620-94-1-0371 and by NSF contract ECS-9412008, and by the State of Florida.

1. E. Spiller, R. Feder, D. Sayre, J. Topalian, D. Eastman, W. Gudat, D. Sayre, Science **191,** 1172–1174 (1976).
2. S. S. Rothman, K. K. Goncz, B. W. Loo, Jr., in *X-ray Microscopy III,* A. G. Michette, G. R. Morrison, C. J. Buckley, eds. (Springer-Verlag, New York, 1992), pp. 373–383.
3. J. R. Gilbert, J. Pine, J. Kirz, C. Jacobsen, S. Williams, C. J. Buckley, H. Rarback, in *X-ray Microscopy III,* A. G. Michette, G. R. Morrison, C. J. Buckley, eds. (Springer-Verlag, New York, 1992), pp. 388–391.
4. D. Rudolph, G. Schneider, P. Guttmann, G. Schmahl, B. Niemann, J. Thieme, in *X-ray Microscopy III,* A. G. Michette, G. R. Morrison, C. J. Buckley, eds. (Springer-Verlag, New York, 1992), pp. 392–396.
5. M. Richardson, K. Shinohara, K. A. Tanaka, Y. Kinjo, N. Ikeda, M. Kado, Proc. SPIE **1741,** 97–104 (1992).
6. P. C. Cheng, S. P. Newberry, H. G. Kim, I. S. Hwang, in *Modern X-ray Microscopies,* P. Duke, A. Michette, eds. (Plenum Press, 1990), pp. 87–118.
7. T. W. Klein, Y. Yoshimasa, H. K. Brown, H. Friedman, J. Leukocyte Biol. **49,** 98 (1991).
8. *Biology of Micro-organisms,* T. D. Brock, M. T. Madigan, J. M. Martinko, J. Parker, eds. (Prentice Hall, NJ, 1988), pp. 60–112.
9. R. M. Bagby, *Histochemistry 69* (1980), pp. 113–130.
10. M. Kado, M. Richardson, K. Gabel, D. Torres, J. Rajyagura, M. Muszyinski, Proc. SPIE **2523,** 194–202 (1993).
11. J. C. Solem, J. Opt. Soc. Am. B **3,** 1551–1565 (1986): R. A. London, M. D. Rosen, J. E. Trebes, Appl. Opt. **28,** 3397–3404 (1989).

CTuD2 **8:30 am**

Measurement and calculation of scattering patterns from cells

Andrew Dunn, Meghan McGovern, Colin Smithpeter, Rebecca Richards-Kortum, *Biomedical Engineering Program—ENS 610, University of Texas, Austin, Texas 78712; E-mail: adunn@mail.utexas.edu*

Knowledge of the optical properties of cells and tissue on the microscopic level is necessary to develop more accurate optical diagnostic methods. Variations in the index of refraction of cellular components are responsible for tissue scattering. Predicting the effects of organelles and other inhomogeneities on scattering is difficult because approximations such as Mie theory cannot be used. We have developed a finite-difference time-domain simulation of Maxwell's equations to compute the scattering patterns of inhomogeneous cells.[1,2] In this work we have measured the scattering pattern of tumor cells and compared the results with the computed patterns. Results indicate that back scattering is primarily due to small-scale spatial variations in the index of refraction of the nucleus of these cells.

A goniometer was constructed to measure the scattering patterns for particles suspended in a cuvette (Fig. 1). A collimated Ti:Sapphire laser beam (λ = 800 nm) was passed through a tank filled with water containing a cuvette; an optical fiber was mounted on an arm that was rotated around the cuvette and the intensity was measured as a function of angle. Measurements of 1-, 4-, and 10-μm diameter polystyrene microspheres showed that the measured patterns were within 10% of the patterns predicted by Mie theory. Because a rectangular cuvette was used, all measurements were scaled to account for Fresnel reflections at the cuvette faces. Late stage tumorous breast cells (MDA-MB 435) were suspended in PBS (10^5 cells/ml). A phase contrast image (400×) of the cells is shown in Fig. 2a. The mean diameter of the cells is 14 μm and the nucleus is 8–10 μm in diameter. The phase contrast image illustrates the variations in optical pathlength and indicates that the nucleus contains small scale fluctuations in refractive index, while the cytoplasm is relatively homogeneous.

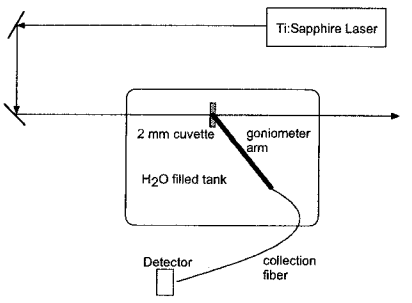

CTuD2 Fig. 1 Experimental goniometer setup.

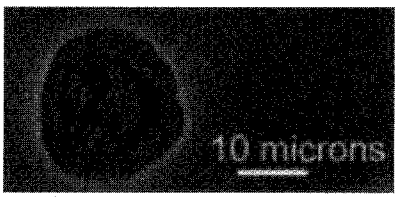

CTuD2 Fig. 2 (a) Phase contrast picture of tumorous breast cells used in the measurements (400× magnification); (b) Cross section of the relative index of refraction of the cell used in the FDTD simulation with nucleus variations. The outermost circle represents the cytoplasm and the inner circle represents the nucleus.

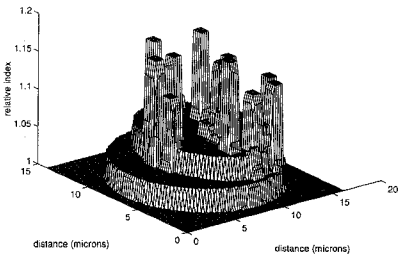

CTuD2 Fig. 3 Comparison of measured and calculated scattering patterns of the tumorous breast cells.

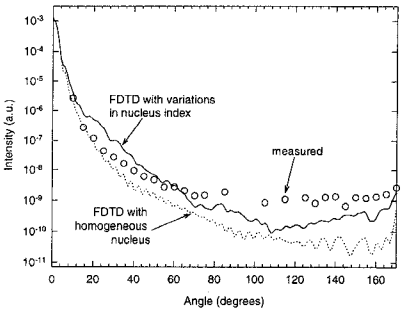

CTuD2 Fig. 4

The FDTD technique, which requires knowledge of the dielectric structure of the cell, was used to compute the scattering pattern of the cell shown in Fig. 2b. The values for the index of refractions were taken from previously published data[3,4] and a spatial variation of about 10% was incorporated into the index of the nucleus. A comparison of the measured and computed scattering patterns for the cell with and without nuclear index variations is plotted in Fig. 3, where the measured intensity has been scaled to the value of the simulated cells at an angle of 10°. At small angles, the measured pattern agrees more closely with the cell containing a homogeneous nucleus, while at high angles the measurements more closely resemble the cell with the inhomogeneous nucleus. These differences demonstrate the need for more accurate measurements of the index of refraction of each cellular component. Based on the results in Figs. 2 and 3, the backscatter level appears to be the result of the index variations in the nucleus of these cells.

The authors thank K. Kline for providing the cells and the High Performance Computing Facility at the University of Texas.

1. K. Yee, IEEE Trans. Antennas Propag. **AP-14,** 302–307 (1966).
2. A. Dunn, C. Smithpeter, A. J. Welch, R. Richards-Kortum, in *Biomedical Optical Spectroscopy and Diagnostics,* Vol. II, 1996 Trends in Optics and Photonics Series (Optical Society of America, Washington, DC, 1996), pp. 50–52.
3. A. Brunsting and P. Mullaney, Biophys. J. **14,** 439–453 (1974).
4. J. Maier, S. Walker, S. Fantini, M. Franceschini, E. Gratton, Opt. Lett. **19,** 2062–2064 (1994).